Published in final edited form as:
Invest Ophthalmol Vis Sci. 2009 September ; 50(9): 4162–4172. doi:10.1167/iovs.08-2861.

Molecular Profiling of Conjunctival Epithelial Side-Population Stem Cells: Atypical Cell Surface Markers and Sources of a Slow-Cycling Phenotype

M. A. Murat Akinci[1], **Helen Turner**[1], **Maria Taveras**[1], **Alex Barash**[1], **Zheng Wang**[2], **Peter Reinach**[2], and **J. Mario Wolosin**[1,3]

[1]Department of Ophthalmology, Mount Sinai School of Medicine, New York, New York

[2]Department of Biological Sciences, SUNY College of Optometry, New York, New York

[3]Black Family Stem Cell Institute, Mount Sinai School of Medicine, New York, New York

Abstract

PURPOSE—Side-population (SP) cells isolated from limbal and conjunctival epithelia derive from cells that are slow cycling in vivo, a known feature of tissue stem cells. The purpose of this study was to define the molecular signature of the conjunctival SP cells and identify markers and signaling pathways associated with the phenotype of these cells.

METHODS—Overnight cultures of freshly isolated human conjunctival epithelial cells stained with Hoechst 33342 were sorted by flow cytometry into SP and non-SP cohorts. Isolated RNA was processed for microarray analysis using a commercial oligonucleotide spotted array. Results were validated at the gene and protein levels by quantitative PCR and immunologic methods. Data mining methods were used to identify cellular processes relevant for stem cell function.

RESULTS—Comparative analyses of transcripts expression based on present and absent software calls across four replicate experiments identified 16,993 conjunctival epithelial transcripts including 10,266 unique known genes of ~24,000 represented in the array. Of those genes, 1254 and 363 were overexpressed (>2-fold) or underexpressed (<0.5-fold), respectively, in the SP. The overexpressed set included genes coding for proteins that have been associated with (1) embryonic development and/or stem cell self renewal (*MSX*, *MEIS*, *ID*, *Hes1*, and *SIX* homeodomain genes); (2) cell survival (e.g., CYP1A1 to degrade aromatic genotoxic compounds); (3) cycling rate (e.g., DUSPs and Pax6 to foster slow cycling); and (4) genes whose expression is not typical in epithelia (e.g., *CD62E*).

CONCLUSIONS—The molecular signature of conjunctival SP cells is consistent with a stem cell phenotype. Their gene expression patterns underpin slow cycling and plasticity, features associated with tissue stem cells. The results provide valuable insights for the preservation and/or expansion of epithelial stem cells.

The ocular surface is lined with two distinct stratified epithelia (E): the limbo-corneal and conjunctival (CNJ) lineages. Similar to many other tissues and organs, their survival and health require that this cell population undergo rapid and constant renewal. This outcome depends on constancy of stem cell function. Only stem cells can generate the whole progeny of a given

Corresponding author: J. Mario Wolosin, Department of Ophthalmology, Mount Sinai School of Medicine, One Gustave L. Levy Place, Box 1183, New York, NY 10029-6574; jmario.wolosin@mssm.edu.

Disclosure: **M.A.M. Akinci**, None; **H. Turner**, None; **M. Taveras**, None; **A. Barash**, None; **Z. Wang**, None; **P. Reinach**, None; **J.M. Wolosin**, None

lineage and simultaneously regenerate new stem cells for future renewal needs. Stem cells from multiple tissues share several functional characteristics including residency within a nurturing niche and the ability to remain in a semi-quiescent state for substantial periods, a feature commonly referred to as slow cycling.[1–3]

Isolation of tissue-specific stem cells to further the study of their molecular composition and functional properties has been a major direction of research in the past few decades. In recent years, several laboratories have reported the isolation of subpopulations putatively enriched in stem cells from the ocular surface.[4–9] The isolation is based on the ability of tissue stem cells to reduce passive accumulation of the amphiphatic DNA-binding dye Hoechst 33342 by increasing its active efflux.[10–12] Cells isolated based on this property were designated side-population (SP) cells.[10] To date, SP cells have been isolated from a large number of tissues and organs. Most of these studies, including those in ocular surface epithelia, have concluded that SP cell cohorts are enriched in tissue stem cells.[11–15] For the bone marrow, some of the SP cell features, primarily being $CD34^-$ cells that can yield a $CD34^+$ progeny, suggest that these cells are at the top of a hematopoietic stem cell hierarchy.[16]

Our studies of limbal and conjunctival cells have shown that rabbit CNJE SPs are highly enriched with cells that are slow cycling in vivo and that, in vitro, display multiple features associated with the epithelial stem cell phenotype, including (1) resiliency to induced differentiation by phorbol esters, a known feature of stem cells in ectodermally derived epithelia, and (2) slow recruitment to proliferation when set in culture.[5]

Using wide-range expression microarrays (HG-U133 plus 2.0; Affymetrix, Santa, Clara, CA), we compared the molecular signature of CNJE SP cells isolated after a short culture period with that of a relevant cohort of non-(n)SP cells. This study demonstrated the highly distinct nature of the CNJE SP cells and led to the identification of unique ocular surface cell proteins and multiple genes that may play a role in controlling stem cell conservative replication, survival capacity, or slow-cycling phenotype.

MATERIALS AND METHODS

Tissue Procurement, Cell Isolation, and Culture

Whole human conjunctivae from unidentified cadavers, aged 55 to 65, were obtained from the National Disease Research Interchange (NDRI, Philadelphia, PA) within 48 hours of collection. No donor details apart from serious pre-mortem disease states, age, sex, and cause of death were released. The use of human tissue in the study was in accordance with the provisions of the Declaration of Helsinki and sanctioned by the Institutional Review Board. Fresh rabbit tissue was obtained from local abattoirs within 1 hour of death. Unless stated otherwise, all reagents were procured from Sigma-Aldrich (St. Louis, MO).

Each conjunctiva was quartered and incubated for 16 to 20 hours at 4°C in a culture flask containing 5 mg/mL Dispase (Roche, Nutley, NJ) dissolved in 4-(2-hydroxyethyl)-1-piperazine-ethanesulfonic acid-buffered (hb), penicillin-streptomycin-complemented Dulbecco's modified Eagle's medium and Ham-F12 1:1 mix (D/F-12) with a slow (20–30 cycles/min) side-to-side tilting motion. At the end of this incubation, the epithelial sheet was essentially separated from the underlying stroma and could be floated into the bathing solution with gentle mechanical prodding. Epithelial sheets were transferred to a 50 mL conical tube containing 15 mL trypsin solution and incubated for 20 to 25 minutes at 37°C under 40 cyc/min orbital agitation. After trypsin neutralization with hbDF/12 complemented with 20% fetal bovine serum (FBS), suspensions were sequentially sieved through 100- and 40-μm filters. Filtrates consisting of almost pure single cells were centrifuged at 200*g*. The cell pellets were resuspended in SHEM consisting of D/F12 complemented with 5% FBS, 10 ng/mL cholera

toxin, 10 ng/mL epidermal growth factor (EGF), and 0.5% dimethyl sulfoxide, plated in 75 cm^2 flasks at a density of 80,000 to 100,000 cells/cm^2, and then cultured overnight (14–16 hours) at 37°C in a 5% CO_2 incubator. For immunostaining, 10,000 cell aliquots were cultured in parallel on printed slide 0.3-mm microwells.

Flow Cytometry

After 10 to 12 hours of culture, the medium was refreshed with prewarmed solution to remove floating cells (60%–70% of total plated) and complemented with 5 μg/mL Hoechst 33342 for 1.5 hours. The treated cells were then released by trypsinization (2 minutes, 37°C), spun down, and resuspended in ice-cold phenol red-free D/F12 complemented with 5% serum and 1 μg/mL propidium iodide (PI). In some experiments, before trypsinization, the Hoechst-incubated cells were incubated at 4°C for 30 minutes with FITC-conjugated mouse monoclonal anti-CD62E antibody (clone 1.2B6; Southern Biologicals, Birmingham, AL) dissolved in ice-cold Hanks' balanced salt solution (HBSS) complemented with 1% BSA. Cell sorting was performed by flow cytometry (Influx; Cytopeia, Seattle, WA). The source tube was maintained at 4°C at all times, and collection solutions were stirred by means of minimagnets and a custom-designed stirrer. For microarray analysis, the cells were collected in 750 μL isolation reagent (Tri-Reagent LS; Molecular Research Center, Cincinnati, OH). For cytospinning, the cells were collected in HBSS complemented with 0.01% BSA. For cell cycle determination, sorted rabbit SP and nSP cells derived from a pool of 10 conjunctivas, were collected in HBSS, fixed with 0.1% formaldehyde, permeabilized with 0.045% Triton X-100, spun down, resuspended in HBSS-+1% BSA+5 μg/mL PI solution and analyzed in a flow cytometer (LSR II; BD Biosciences, Franklin Lakes, NJ). Two thousand SP or nSP cells were cytospun onto slides with a modified narrow-diameter (0.2 cm) chamber. Spun-down cells were fixed in −20°C methanol and air dried.

Microarray Processing

Two conjunctivas from a single donor were used in each microarray experiment. Isolation solutions containing the collected SP and nSP cell volumes were adjusted to 1.0 mL by the addition of H_2O and 0.5 μL polycryl RNA carrier (MRC). RNA was isolated according to the manufacturer's instructions. Purified RNA was dissolved in 5 to 4 μL water, and 0.5 mL was used to determine RNA yield with an RNA quantitation reagent (Ribogreen; Molecular Probes, Eugene, OR). Each 1000 sorted cells yielded 1.5 to 2.2 ng RNA. RNAs were adjusted by either addition of water or evaporative concentration to an identical concentration and volume, converted into cDNA (SuperScript Choice reverse transcriptase; Invitrogen-Gibco, Bethesda, MD) and a modified oligodT primer (Affymetrix). The initial cDNA underwent two cycles of in vitro transcription (ENZO BioArray HighYield Kit; Affymetrix) to generate biotin-labeled amplified cRNA. Appropriately fragmented (restricted) biotin-labeled cRNA was hybridized to gene oligonucleotide microarrays (HG-U133 plus 2.0; Affymetrix) according to the manufacturer's protocol. The HG-U133 plus 2.0A array contains more than 38,000 unique GenBank (maintained by the National Center for Biotechnology Information, Bethesda, MD) accession numbers (genes) arranged in ~55,000 probe sets. Hybridized microarrays were stained with a streptavidin-phycoerythrin reagent, and fluorescence images were captured with a laser scanner (G2500A; Agilent, Santa Clara CA).

Data Processing and Analyses of Differential Gene Expression

Signal intensities (SIs) and signal quality properties were extracted from the fluorescent images (Microarray Suite, ver. 5.0 [MAS 5.0]). The normalized SI for each transcript and the P/A/M calls reflecting the chances that the SI is a true (P, present), a false (A, absent), or a marginal (M) positive, were collected in spreadsheet format for downstream processing. These primary normalized signal intensities have been deposited in the NCBI Gene Expression Omnibus

(GEO, http://www.ncbi.nlm.nih.gov/geo/ provided in the public domain by the NCBI, Bethesda, MD) and are accessible through GEO Series accession number GSE12631. Annotation data were obtained from NetAffix (Affymetrix).

To establish a list of all expressed transcripts for the cultured CNJE, we processed the spreadsheet file according to the following rules. A transcript was considered expressed when it did not receive an A call in any of the four replicates and when there was not more than one M call (e.g., P, P, M, and P for the first through the fourth experiments). All transcripts complying with this requirement in at least one of the two cell types (SP and nSP) were grouped in a single transcript list: the all-expressed transcript list. A differentially expressed transcript list was derived from the all-expressed list by including only those transcripts for which, the SP average SI divided by the average for the nSP was higher than 2.0 (SP overexpressed) or lower than 0.5 (SP under-expressed), provided that, in addition, the SP/nSP SI ratio within each of the four paired comparisons was either higher than 1.50 or lower than 0.66. This empiric filtering method was chosen because the use of statistical approaches is not truly justified, since our experimental sample ($n = 4$) could not be a full representation of a human population for all genes. The SI ratio filter was waived for those transcripts that had a PPPP/AAAA MAS 5.0 call distribution. From the all- and differentially expressed transcript lists, we generated corresponding lists of known genes, the all-expressed (AE) and differentially expressed (DE) gene lists, respectively, by removing ESTs and other nonannotated entries and by choosing the transcript that yielded the highest SI for a given gene when more than one transcript representing a single gene existed. In all cases examined, this transcript represented the sequence closer to the 3′ (polyA) end of the gene.

The Database for Annotation, Visualization, and Integrated Discovery (DAVID; http://david.abcc.ncifcrf.gov/ provided in the public domain by the National Institute of Allergy and Infectious Diseases [NIAID], Bethesda, MD), was used to identify overrepresented entities and biological or molecular processes within the differentially expressed transcripts. DAVID analysis probes each gene list against the corresponding population lists and calculates scores (*P*-values) for the likelihood of overrepresentation in multiple ontological systems derived from a variety of public genomic resources including the Gene Ontology (GO) and Protein Information Resource (PIR) consortia. The Gene Map Annotator and Pathway Profiler (GenMAPP; http://www.genmapp.org/; provided in the public domain by the Gladstone Institute, University of California San Francisco) was used to explore and develop graphic representations of genes differentially expressed in the SP cells in the context of selected signal transduction pathways.

Quantitative PCR

The SP cell yield from a single donor, ~12,000 cells, and a matched amount of nSP cells were isolated and collected (Tri-Reagent-LS; Molecular Research Center). One half of the total RNA purified from these collections (~15 μg) was used to generate ~1 μg preamplified cDNA (Full Spectra RNA Amplification kit; SBI, Mountain View, CA) and the other half was processed in parallel with omission of reverse transcriptase. Enzyme omission resulted in complete absence of DNA product. PCR reactions were performed in triplicate wells in 384-well plate sequence-detection system (Prism 7900HT PCR system; Applied Biosystems, Inc. [ABI] Foster City, CA) using the SYBR Green master mix (RT^2 SYBR Green/ROX PCR Master Mix; SuperArrays, Frederick, MD), 5 ng amplified DNA per well and qPCR primer pairs (RT^2 primer pairs; SuperArrays; ABI). Because these primers are proprietary sequences, we used agarose gel chromatography to verify that the reaction products matched the base pair length information provided by the manufacturer (not shown). SP/nSP RNA ratios in the amplified material were calculated from cycle thresholds (C_ts) according to the Δ of ΔC_t method using β-actin for normalization.

Immunostaining

Cell cytospins, cells cultured on printed glass slides and cryostat sections of embedded human conjunctivas (Cryomatrix; Shandon, Pittsburgh, PA), were immersed in cold methanol for 10 minutes, air dried, rehydrated in phosphate-buffered saline (PBS), blocked for 15 minutes in PBS-4% BSA, and reacted with rabbit polyclonal against CD62E (NeoMarkers, Freemont, CA), mouse monoclonal antibodies against CD62E (clone 1.2B6; Abcam, Cambridge, MA) or DUSP4 (clone 48; BD-Transduction Laboratories, San Jose, CA) and mono (clone AE1/AE3, Fitzgerald, Concord, MA)- or poly (Biomedia, Singapore)-clonal, pan-cytokeratin, or keratin 14 (FITC-conjugated; Abcam) for 45 minutes. After three washes in Tween 20-PBS, the specimens were overlaid with the appropriate Alexa Fluor 488- or Alexa Fluor 568–conjugated goat anti-rabbit or anti-mouse IgGs (all from Invitrogen) for 45 minutes, washed for 16 hours at 4°C in PBS, mounted in a 1:4 mixture of antifade medium (Vectashield; Vector Laboratories, Burlingame, CA) and 90% glycerol and examined and photographed with an epifluorescence microscope. In some cases, the cell nuclei were counterstained with either DAPI or PI.

For immunoblot analysis, rabbit cells were denatured in Western blot sample buffer at a density of 10^3 cells/μL, chromatographed in polyacrylamide gels, transferred to nitrocellulose membranes, and reacted with antibodies against phosphorylated ERK1/2 (p-ERK). Subsequently, a membrane was incubated with HRP-conjugated goat anti-mouse IgG, and finally the amount of bound HRP activity was revealed by autoradiography. Membranes were then stripped of staining reagents and restained by using the same procedures with either an anti-ERK1/2 or anti-β-actin Abs followed again by the secondary HRP-conjugated Ab. All immunoblot Abs were from SCBT (Santa Cruz, CA).

RESULTS

Cell Culture and Cell Sorting

RNA yields from SP and nSP cells sorted directly from freshly trypsinized cell suspensions were only 0.1 to 0.4 pg/cell and their RNA quality was extremely poor (Wolosin JM, unpublished, 2006). This result may be due to the prolonged trypsinization needed to dissociate this epithelium, compounded by the inclusion of the anchoring-dependent epithelial cells in suspension. To surmount this intrinsic barrier to the molecular characterization of SP cells of solid tissues, we cultured the conjunctival cells at <100,000 cells/cm^2 before cell sorting. Costaining for total keratin and keratin 14 after a 12-hour culture showed that approximately 97% of the adherent cells were bona fide epithelial (pan cytokeratins positive) cells and approximately 70% were positive for the basal cell keratin 14 (not shown). The effect of the time in culture on SP cell abundance was investigated using both rabbit and human conjunctivas (Fig. 1). Based on preliminary investigation, the analysis was performed using light-scattering gates that exclude the majority of cells of nonepithelial lineages.

In the rabbit, SP cells, ~1.6% of adherent cells at 16 to 24 hours (average for five independent experiments), decreased rapidly afterward and were essentially null by the third day (Figs. 1A–C). The decreases appear to be linked to cell proliferation: when cells were seeded in serum and growth factor–free medium (D/F12 and 1% BSA) SP yields were preserved (Figs. 1D, 1E). The SP yield for human cells cultured in SHEM, however, remained constant for the first 48 hours (Figs. 1E–G). Cell cycle analysis of rabbit SP cells (the number of cells needed to complete this two-stage experiment preempted its completion with human cells), isolated from a pool of six rabbit conjunctivas, showed that at the time of collection, at least 99% of the SP cells (two experiments) were in G_0/G_1 (Fig. 2). Hence, the nSP was taken from the center of the G_0/G_1 Hoechst image as indicated in Figure 1F.

Quality Controls

Adherent cell yields per human conjunctival pair (single donor) were typically 2 to 3 million cells. The light-scattering gate-restricted SP cohort accounted for approximately 0.3% to 0.5% of the human conjunctival epithelial adherent single cell population, or 6,000 to 12,000 SP cells. The average RNA yields for the sorted cells ($n = 4$) were 2.6 and 2.4 pmol/cells for the SP and nSP populations, respectively or between 15 to 30 ng/per experiment. These limited quantities of RNA hindered measurements of RNA purity or origami integrity. This problem was particularly important in this study because the need to trypsinize adherent cells and maintain them in suspension until and during sorting could cause some RNA degradation. Hence, we relied on the quality control probes included in the microarray (HG-U133A plus 2.0; Affymetrix) to generate a robust retrospective analysis of the effect of the cellular processing used on the final quality of the microarray results.

The microarray contains three distinct probes for glyceraldehyde-3 phosphodehydrogenase (*GAPDH*), each representing distinct sections of the gene in the 5′ to 3′ (polyA) direction. A fourfold decrease in the SI for the 5′ end probe (1000 bp away from the polyA) relative to the 3′ end probe (Table 1A) suggests that some degradation occurred in the course of cell sorting. Nevertheless, such a partial degradation is likely to have had minimal impact on our comparative analysis for two reasons: The degree of degradation was similar for both SP and nSP samples so that the SI ratios for probes that are as much as 1000 base pairs away from the polyA site is the same as for the 3′ end probes, and in fact, unlike the case for *GAPDH*, where probes spanning the whole length of the message were intentionally included in the microarray for quality control, for nearly all the genes, the microarray includes at least one probe derived from the polyA-proximal (3′ end) of the sequence. RNA equivalence is also supported by the similar percentage of present calls in the two populations (Table 1B).

Finally, an examination of SI values and P/A calls for nonepithelial markers (Table 1C), demonstrated that the collected SP and nSP populations were essentially free of the three nonepithelial cells most commonly found within the conjunctival epithelial strata, hematopoietic (CD45), antigen presenting dendritic (CD1), and melanin-producing (tyrosinase) cells. Conversely, the average levels of expression for all 24 intermediate filament genes expressed in the tissue were very similar in the two populations.

Global Differential Gene Expression Analysis

The AE gene list contained 10,265 unique genes or approximately 40% of all the unique annotated genes represented in the array. Of these 10,265 AE genes, 1,617, or approximately 16%, were differentially expressed. This high percentage indicates that the SP cells are markedly different from the generic G_0/G_1 basal cells represented by the nSP cohort. Of the 1617 genes, 1254 were SP overexpressed and 363 underexpressed (i.e., a more than 3:1 ratio). This large asymmetry can be visualized in a plot of SI values (average for the SP and nSP) versus $\log_2$ of the ratio between the SP and nSP SIs for the whole AE list (Fig. 3, main frame). The SP cells seem to overexpress a very extensive set of genes of low to moderate SI. Since the microarray results were normalized to identical total expression (sum of SIs for SP = sum of SI for nSP), the excess expression in the SP decreased the relative weight of high-expression genes, mostly invariant housekeeping genes. As a result, these genes appeared to have SP/nSP ratios below 1 (e.g., *GAPDH*, see Table 1). The equivalent plot for the nonpresent transcripts (i.e., mostly random false-positives) was essentially symmetric around the *y*-axis (Fig. 3, inset), indicating that the expression asymmetry did not represent an artificially generated bias.

The microarray expression ratios for 10 genes were subjected to independent validation by qPCR (Table 2). The small amount of RNA collectable per experiment made it necessary to preamplify the cDNA. Given the implicit risk of nonlinear amplification, in particular since

the amount of RNA imputed was well below the amount suggested by the manufacturer, the PCR results cannot be viewed as truly quantitative. Nevertheless, the qualitative concordance obtained provides general validation of the microarray ratios.

Table 3 displays the most prominent SP overexpressed and underexpressed genes. The lists include genes involved in multiple unrelated cellular activities. No single central or dominant cellular function is readily identifiable, but there are many intriguing genes for future analysis and more detailed delineation of the SP cell phenotype.

Cell Surface Markers

One of the most valuable results from a differential global gene expression study is identification of exclusive cell surface markers, as such markers facilitate minimally intrusive tracking and isolation of the cell of interest in the viable state. The gene with the highest SP/nSP SI ratio represented CD62E/E-selectin (Table 3). The presence of this gene in the CNJE was surprising. CD62E, a cell surface protein involved in leukocyte adhesion, is thought to be expressed only in activated vascular endothelia.[17] Nevertheless, consistent with the microarray results, staining of cytospun SP and nSP CNJE with anti-CD62E antibodies identified a highly expressed epitope in the cell surface of most SP cells, but not in the nSP population (Fig. 4A) and costaining of 12-hour cultures with anti-CD62E and keratin 14 Abs proved that the expression occurred in basal epithelial cells (Fig. 4 B). After 72 hours of culture, when the cells had spread, migrated, and proliferated, cytokeratin-rich CD62E cells with classic epithelial morphology could be seen intercalated between CD62E-negative cells (Figs. 4D, 4E). Most of these $CD62E^+$ cells were isolated. In two rare cases, though, we observed adjacent $CD62E^+$ cells of identical stain intensity suggestive of derivation from a proliferation event. In tissue sections, we infrequently identified CD62E staining in well-defined intracellular granules (Fig. 4C). Unlike the case for CD62E, three other endothelial surface proteins CD62P/P-selectin, CD31/P-CAM and CD54/ ICAM-1, were not identified in the microarrays or, at the protein level, by immunostaining (not shown).

The third overexpressed gene in Table 3, *CD93*/*Cq1R* also represents a cell surface protein present in the myeloid lineage with no previous association with epithelial cells.[18] It has been identified as a marker for myeloid and hepatic-yielding stem cells.[19] The fifth gene in Table 3, *CXCR4*, is a widely expressed, pleiotropic cytokine receptor that may have critical roles in stem cell function throughout mammalian lineages.[20] Detailed results on the expression of these and other surface proteins in the CNJE cells and the relationship between them and the SP phenotype will be presented elsewhere (Wolosin et al., manuscript in preparation).

Categorical Analysis

DAVID analysis of the overexpressed and underexpressed SP gene lists identified overrepresented terms within various on-tologic classifications. The terms with highest significance for each case are presented in Table 4. Functional clustering in relational groups, redundant categories in different ontological systems, and terms describing the most general categories (e.g., regulation of cellular metabolism), have been excluded. The overrepresented categories in the overexpressed gene set indicates that, in these short-term cultures, SP cells are uniquely involved in intense transcriptional activity, principally through C2H2 zinc finger transcription factors. Overrepresentations within the underexpressed gene set suggest that, in comparison to the general nSP cell population, SP cells are particularly underequipped for motility and migration (e.g., actin cytoskeleton) and spreading (e.g., intracellular protein traffic).

Topical Analysis and Cell Cycle Pathways

To identify potentially significant features of the SP cells that may depend on a few pivotal genes and hence would not be highlighted by the overrepresentation analysis, we scanned the DE list for a few specific gene categories, including (1) homeodomain genes that have been implicated in either stem cell renewal or in development, (2) genes that may contribute to slow or infrequent cycling, and (3) genes that may help with cell survival. Selected results of these studies are shown in Table 5. The first gene in this table, *MSX1*, is involved in regulating cellular plasticity. Its ectopic expression inhibits the differentiation of a variety of mesenchymal and epithelial progenitor cell types and reverses myotubal differentiation.[21,22] Another overexpressed gene, *MEIS1*, has been shown to enhance expansion of the pools of hematopoietic precursors.[23] Two other homeodomain morphogenes that are critical for eye development, *PAX6* and sina oculis1 (*SIX1*) were also highly overexpressed. *PAX6* is highly expressed in the ocular surface epithelia and may contribute to the stem cell phenotype as a proliferation moderator.[24]

The highly overexpressed *HES1* and *ID* genes act as dominant negative blockers for the differentiation-inducing helix-loop-helix proteins. *HES-1* expression preserves purified hematopoietic cells ex vivo and augments the hematopoietic SP cell population in vivo.[25] *ID1* is critical for long-term repopulating hematopoietic stem-cell maintenance.[26] In fact *HES1* and *ID1* expression may be interrelated. During development, *HES1* expression is enhanced by *ID* product activity.[27]

Within the stem-cell–related canonical WNT/β catenin/ TCF pathway,[28,29] the DE gene list included only two genes, *Wnt9* and *Wnt8B*, and only the latter had a very moderate twofold increase expression in the SP. In addition, SP-nSP expression differences were not observed for the frizzled (FZD) receptors for these ligands. However, SP cells strongly underexpressed DKK1 and DKK3, main antagonists of the canonical WNT/β catenin pathway.[30] Low levels of DKKs may facilitate WNT signaling in the SP respective to the signal strength in the DKK-high nSP cell. SP cells have augmented levels of the noncanonical *WNT5A* gene and of its receptor, FZD5. The pathways associated with, and effects of noncanonical WNTs are poorly understood.[31] When acting as an inhibitor, *WNT5A* has been shown to foster a slow-cycling status that stabilizes the hematopoietic stem cell phenotype.[32] Furthermore, WNT5a may act as an activator or inhibitor of the (canonical) β catenin/TCF signaling depending on receptor context.[33] Hence, the noncanonical classification of Wnt5a does not preclude a relevant role for this gene in these epithelial stem cells.

Systems that may regulate premature apoptosis or determine cell survival under challenging conditions were also examined. Annexin A1, one of the most SP-overexpressed genes (Table 3A; SP/nSP ratio, 12.55) is a pleiotropic blocker of inflammatory mediator release.[34] Members of the type 2C ser/threo protein phosphatase family, a set of enzymes that seem to negatively regulate cellular stress signaling, also displayed substantial overexpression. The most overexpressed family members, PPM1D (Table 3A) and PPM1H (ratio, 6.94) has been shown to attenuate oxidative stress-induced phosphorylation of p38 MAP kinase in epithelial cells.[35] But, seemingly more significant, *PPM1D*, also called *Wip1*, for wild type 53-induced phosphate-1, has been shown to increase the threshold for an apoptotic response to DNA damaged through its role in the p53-Mdm2 autoregulatory loop.[36,37] SP cell protection from oxidative damage to DNA may be afforded by the high overexpression of CYP1A1 (Table 3A), a dioxin-inducible enzyme that degrades aromatic genotoxic compounds.[38] Polymorphisms in this gene correlate with increased incidence of cancers.[39] Within the complement cascade, substantially overexpressed genes were limited to complement factors CFB (SI, 3534; ratio, 5.64) and CFH (SI, 2122; ratio, 4.57). These two factors ensure that the complement system is directed toward pathogens and does not damage host tissue.

Polymorphisms of these genes have a high correlation with age-related macular degenerations.[40,41]

The nature of the genes with the highest SP underexpression in Table 3B (nSP SI>>SP-SI) is consistent with the results of DAVID analysis indicating paucity of cell components related to cell motility and migration in the SP cells.

In addition to the topical analysis, GenMapp was used to generate maps of a large number of intracellular pathways and gene clusters (http://cgap.ncbi.nih.gov/pathways; provided in the public domain by the National Center for Biotechnology Information). While the interpretation of the significance of individual gene expression differences in many of these maps was not apparent or given to unambiguous interpretation, all the pathways associated or affecting activity at the cell cycle restriction (R) point that control transition from late G_1 to S, namely (1) the mitogen activated kinase (MAPK) cascades (GenMapp's file Hs_MAPK_signaling_pathway_KEGG); (2) the cyclin D associated kinases (GenMapp's Hs_Cell_cycle_KEGG); and (3) TGFβ (GenMapp's Hs_TGFβ_KEGG) yielded readily interpretable images on unique features of the CNJE SP cell (Fig. 5).

To build Figure 5, it was necessary to ascribe MAPK (i.e., ERK1/2, p38 or JNK) specificity to MAPK phosphatases. This attribution was made on the basis of recently published data on MAPK-MAPK-phosphatase interplay showing that (1) DUSP5 and DUSP6/MKP3 are, respectively, nuclear and cytosolic phosphatases wholly selective for ERK enzymes[42–44]; (2) DUSP1 and DUSP4 are nuclear phosphatases that can deactivate enzymes from all three branches of the MAPK cascades[45,46] and can block ERK-dependent proliferation, but, due to differences of affinities for the kinases representing each of the three branches of the cascade,[47] DUSP1 and/or DUSP4 may not be effective in many instances as ERK function blockers.[48–50]

For the MAPK pathways (Fig. 5, left side) the most significant facts are that (1) there are only nominal changes in the aggregate expression levels of all MAPK isoforms comprising each of the three terminals kinase nodules: ERK (~25% lower in the SP), p38 (20% higher in the SP), and JNK (25% lower in the SP); (2) the dual specificity phosphatases (DUSPs) the only enzymes that are available to dephosphorylate and thereby inactivate the ERK, p38, and JNK enzymes, in particular the ERK-specific DUSP5, are substantially overexpressed in the SP cells. Our qPCR measurements validated the microarray results for DUSP 4, -5, and -6 at the gene level (Table 2). In addition, DUSP4 immunostaining of sorted cytospun cells validated the result for this gene at the protein level (Fig. 6). The stain was acutely localized to the nuclei and the fluorescence intensity in the SP nuclei was 3.4 times higher than that of nSP cells (average value for 15 cells of each). Remarkably, a similar multi-DUSP overexpression has been observed in keratinocyte SP cells.[51]

The large overexpression of DUSPs imply dramatic changes in absolute kinase/kinase phosphatase gene ratios. The (MAPK1/ERK)/(DUSP5+DUSP4+DUSP6) SI quotient decreased 15 times, from 5469/716 to 4413/9163 (SIs for MAPK3/ERK1 measured in the microarray are very low). Including DUSP1 in the analysis does not radically modify this calculation. For the other two branches of the MAPK cascades, p38 and JNK. Similar calculation using MAPK13+MAPK14 for p38 and MAPK8+MAPK9+MAPK10 for JNK and dividing by DUSP1+DUSP4 (DUSP5 and -6, are ERK specific) yielded SI quotient decreases of six- and fivefold, respectively. Such large changes could be expected to prevent establishment of a phosphorylated MAPK state in SP cells and hence, attenuate or completely block SP cell responses to mitogenic and/or migration-inducing and inflammatory inputs.

To test this hypothesis, we cultured a large batch of rabbit CNJE cells in growth factor-free (base) medium for 24 hours, sorted equal amounts (80,000) of SP and nSP cells into the same

base medium and determined EGF induction of ERK phosphorylation by Western blot analysis. A representative result from three independent trials is shown in Figure 6; ERK phosphorylation was never detected in the SP cells. Not directly predictable from the human microarray results, in the rabbit total ERK protein was markedly reduced in the SP cells. For p38, SP phosphorylation was detectable but at a much lower level than that for the nSP cell (not shown).

Figure 5 also incorporates the expression of CXCL12/SDF-dependent CXCR4 (Table 3A). The SDF-CXCR4 interaction enhances skin wound healing and clonogenic growth of keratinocyte precursors in vitro.[52,53] *CXCR4* downstream signals include activation of PI-3 kinase and *RAS*. The latter is one of the early genes in the mitogen activated ERK cascade (Fig. 5). Hence, the very large *CXCR4* overexpression in the SP may provide a SP cellular activation that is synergetic with the EGF-initiated ERK activation.

The right side of Figure 5 focuses on the TGFβ/TGFβ-like (activin) receptor pathway. The primary effect of TGFβ in ectodermally derived epithelial cells is cell cycling arrest. The arrest is secondary to phosphorylative activation of the nuclear p-type kinase inhibitors of cyclin D (Fig. 5). In the extracellular/cell membrane domain of the pathway the microarray analysis reveals only moderate changes in gene expression of TGFβs and TGFβ receptors (Table 5). However, SP cells showed a marked underexpression of the follistatin (*FST*) gene. Follistatin is a secreted protein that sequesters and thereby neutralizes activins.[54,55] The low FST expression (nSP/SP ratio, 0.11) could render the SP cell to be highly sensitivity to TGFβs.

Within the nucleus, there were further differences in SP-nSP gene expression patterns that are highly meaningful for cyclin D system function. First, SP cells underexpressed the cyclin D kinases (CDK4 and 6) responsible on association with cyclin D isoforms for activating retinoblastoma, the final stage in releasing cells from the G_1 to the S phase of the cell cycle. Second, this negative effect of cyclin kinase deficiency on cell cycle progression is compounded by the overexpression of several cyclin-dependent kinase inhibitors, which specifically act on the cyclin D/cyclin D kinase complexes. It is noteworthy that, in contrast to the marked differences in CDK4 and -6, other kinases associated with other regulation points of the cell cycle showed no major expression differences. For instance, cyclin A-associated p21 shows minimal differences (Fig. 5) and of 17 cell division cycle (CDC) kinases identified in the microarray 15 are unchanged, 1 was overexpressed 2.6 times and 1 was underexpressed 2.5-times.

Finally, two cytokeratins that have been linked to the stem/precursor cell phenotype in epidermis, K15 and -19,[56] were also part of the SP-overexpressed gene set (ratios of 3.78- and 3.38-fold, respectively). Yet, at the same time, expression of the basal cytokeratin K14 was substantially underexpressed in SP cells. This is a seemingly surprising finding although it has also been observed in epidermal SP cells.[15]

DISCUSSION

In this study, we compared SP and nSP cells gene expression profiles after a brief culture period. The approach selected a population consisting mostly of undifferentiated, adherent cells and ensured that these cells were exposed to Hoechst 33342 in an optimal metabolic state, a critical factor for the energy-dependent efflux of Hoechst and for recovery of RNA integrity.

Our results clearly establish that conjunctival epithelial SP cells have properties that are uniquely different from those described for the far more numerous adherent (nSP) population. Genes differentially expressed in stem/precursor cells are expected to reflect their unique features such as self renewal, adhesion, or chemoattraction to a unique niche and survival capabilities. Nevertheless, because the culture conditions used in our study cannot fully

duplicate the essential niche environment, the SP cell gene expression profile described herein may differ from that existing in vivo. Therefore, the actual role of each differentially expressed gene must be interpreted with caution. In developmental processes, short transient expression of highly specific genes commonly underpins cell fate events. Likewise, early differentiation events triggered by the culture environment may lead to expression of differentiation-related genes at higher levels in the SP cells than in the generic nSP cell population used as the non–stem cell control. Finally, it should be stressed that the tissue collection protocol did not (and could not) control the health status of the donor conjunctiva. Chronic conjunctivitis, rheumatism, or dry eye in some of the donor tissues may have modified the gene expression pattern from that existing in the normal condition.

The overrepresentation analysis suggests that a large number of transcription factors, in particular those belonging to the C2H2 zinc finger protein subtype, may underpin the overall gene overexpression in the SP cells. Presently, the information available on either upstream control of the expression of these DNA transcription regulators or their site of action is not sufficient to develop cogent transcription factor–specific gene correlations.

Research in the hematopoietic system, in keratinocytes and in the gastrointestinal track has identified the Wnt, Notch, and Hedgehog signal transduction pathways as potential players in the stem cell renewal event that may be needed for ex vivo stem cell expansion.[57–59] The present results provide a primer for further exploration of development-related genes, including members of the MSX, MEIS, DKK, ID, PAX, and SIX homeodomain gene families, whose role may have to be understood to attain CNJE stem cell expansion in culture.

The cultured SP cells expressed, in a highly preferential manner, surface proteins that are rare or atypical for epithelia, in particular CD62E/E-selectin. CD62E is assumed to be present only in cytokine-activated endothelial cells. However, expression of CD62E has recently been reported in the nestin-positive epithelial stem cells isolated from the pancreatic duct and in mesenchymal stem cells from placenta or bone marrow.[60,61] The functional role of CD62E is to bind to Lewis family carbohydrates found on the surface of circulating leukocytes and thereby help recruit these cells at injury sites. It is difficult to derive with this limited information a hypothesis for its potential role in epithelium. One intriguing possibility is that the same cells express a Lewis family epitope. It this is the case, it would provide a mechanism for homologous cell–cell interactions. Alternatively, this expression may result from an intrinsic cellular plasticity and thus be inconsequential for the in vivo condition. In any event, this unique expression may provide the means to isolate by fast and minimally invasive immunopanning a cell population highly enriched in stem-related SP cells.

Adult tissue stem cells have proven highly refractory to expansion and long-term propagation in culture.[62] The pathway analyses of the MAPK, TGF-β, and cyclin cascades suggests that in regard to ocular surface epithelial stem cells, ex vivo cell proliferation may be strongly suppressed by the slow cycling nature of epithelial stem cells in vivo. Using the numerically convenient rabbit cells, we demonstrated that freshly isolated SP cells were highly quiescent. Consistent with this phenotype, the gene analysis of human SP cells reveals cellular signaling pathway patterns that seem to be aimed at blocking proliferation. The large DUSP overexpression in the human SP cells can be expected to maintain ERK in a dephosphorylated state, preventing their transit through the restriction point between the G_1 and S phases.[45] The G_1 to S restriction-point activity is likely to be negatively affected in the SP cell by the inhibitory effects of TGF-β that, in these cells may be enhanced by the combination of three distinct expression differences, minimal expression of the TGF-β blocker follistatin, substantial overexpression of p-type cyclin D inhibitors, and underexpression of restriction point cycling kinases (Fig. 5). Of interest, the SP cells overexpressed EGF (Fig. 5). This could result in a

unidirectional paracrine signal, where SP cells foster the proliferation of neighboring nSP cells while blocking their own activation through the DUSP blockade.

If the hypotheses rendered in this analysis is experimentally confirmed through ectopic gene alterations, extracting the full potential of these stem cells through ex vivo stem cell expansion will necessitate identification of the biological cues that elicit the adverse gene expression patterns suppressing proliferation. Should the gene expression patterns observed in the human conjunctiva occur also in the limbal-corneal lineage, advances in this area may be particularly important for improving autologous limbal epithelial stem cell transplantation protocols with cells derived from a healthy contralateral limbus. [63,64] In this respect, it is reassuring that the two more overexpressed cyclin D kinase inhibitors in our study, p15 and p57, are the same ones that show strong TGFβ-dependent upregulation in limbal epithelial cells and that their ablation is sufficient to abrogate TGFβ-induced proliferation arrest.[65]

Acknowledgments

The authors thank the Flow Cytometry, Microarray, and Real-Time PCR shared facilities of the Mount Sinai School of Medicine, without whose help the study could not have been conducted.

Supported by National Institutes of Health (NIH) Awards EY014878 (JMW), EY015132 (JMW), EY04795 (PR) and EY01867 (Core Center Grant) from NIH and an Unrestricted grant from Research to Prevent Blindness, Inc.

References

1. Leblond CP. The life history of cells in renewing systems. Am J Anat 1981;160:114–158. [PubMed: 6168194]
2. Potten CS, Loeffler M. Stem cells. attributes, cycles, spirals, pitfalls and uncertainties: lessons for and from the crypt. Development 1994;110:1001–1020. [PubMed: 2100251]
3. Schofield R. The stem cell system. Biomed Pharmacother 1983;37:375–380. [PubMed: 6365195]
4. De Paiva CS, Chen Z, Corrales RM, Pflugfelder SC, Li DQ. ABCG2 transporter identifies a population of clonogenic human limbal epithelial cells. Stem Cells 2005;23:63–73. [PubMed: 15625123]
5. Budak MT, Alpdogan OS, Zhou M, Lavker RM, Akinci MA, Wolosin JM. Ocular surface epithelia contain ABCG2-dependent side population cells exhibiting features associated with stem cells. J Cell Sci 2005;118:1715–1724. [PubMed: 15811951]
6. Epstein SP, Wolosin JM, Asbell PA. P63 expression levels in side population and low light scattering ocular surface epithelial cells. Trans Am Ophthalmol Soc 2005;103:187–199. [PubMed: 17057802]
7. Wolosin JM. Cell markers and the side population phenotype in ocular surface epithelial stem cell characterization and isolation. Ocul Surf 2006;4:10–23. [PubMed: 16669522]
8. Umemoto T, Yamato M, Nishida K, Yang J, Tano Y, Okano T. Limbal epithelial side-population cells have stem cell-like properties, including quiescent state. Stem Cells 2006;24:86–94. [PubMed: 16150918]
9. Park KS, Lim CH, Min BM, et al. The side population cells in the rabbit limbus sensitively increased in response to the central cornea wounding. Invest Ophthalmol Vis Sci 2006;47:892–900. [PubMed: 16505021]
10. Goodell MA, Brose K, Paradis G, Conner AS, Mulligan RC. Isolation and functional properties of murine hematopoietic stem cell that are replicating in vivo. J Exp Med 2006;183:1797–1806. [PubMed: 8666936]
11. Zhou S, Schuetz JD, Bunting KD, et al. The ABC transporter Bcrp1/ABCG2 is expressed in a wide variety of stem cells and is a molecular determinant of the side-population phenotype. Nat Med 2001;2 (7):1028–1034. [PubMed: 11533706]
12. Zhou S, Morris JJ, Barnes Y, Lan L, Schuetz JD, Sorrentino BP. Bcrp1 gene expression is required for normal numbers of side population stem cells in mice, and confers relative protection to mitoxantrone in hematopoietic cells in vivo. Proc Natl Acad Sci U S A 2002;99:12339–12344. [PubMed: 12218177]

13. Ono M, Maruyama T, Masuda H, et al. Side population in human uterine myometrium displays phenotypic and functional characteristics of myometrial stem cells. Proc Natl Acad Sci U S A 2007;104:8700–8705.
14. Hoshi N, Kusakabe T, Taylor BJ, Kimura S. Side population cells in the mouse thyroid exhibit stem/progenitor cell-like characteristics. Endocrinology 2007;148:4251–4528. [PubMed: 17584961]
15. Redvers RP, Li A, Kaur P. Side population in adult murine epidermis exhibits phenotypic and functional characteristics of keratinocyte stem cells. Proc Natl Acad Sci U S A 2006;103:13168–13173. [PubMed: 16920793]
16. Goodell MA, Rosenzweig M, Kim H, et al. Dye efflux studies suggest that hematopoietic stem cells expressing low or undetectable levels of CD34 antigen exist in multiple species. Nat Med 1997;3:1337–1345. [PubMed: 9396603]
17. Bischoff J, Brasel C, Kräling B, Vranovska K. E-selectin is upregulated in proliferating endothelial cells in vitro. Microcirculation 1997;2:279–287. [PubMed: 9219220]
18. Ikewaki N, Kulski JK, Inoko H. Regulation of CD93 cell surface expression by protein kinase C isoenzymes. Microbiol Immunol 2006;50:93–103. [PubMed: 16490927]
19. Danet GH, Luongo JL, Butler G, et al. C1qRp defines a new human stem cell population with hematopoietic and hepatic potential. Proc Natl Acad Sci U S A 2002;99:10441–10445. [PubMed: 12140365]
20. Ratajczak MZ, Zuba-Surma E, Kucia M, Reca R, Wojakowski W, Ratajczak J. The pleiotropic effects of the SDF-1-CXCR4 axis in organogenesis, regeneration and tumorigenesis. Leukemia 2006;20:1915–1924. [PubMed: 16900209]
21. Hu G, Lee H, Price SM, Shen MM, Abate-Shen C. Msx homeobox genes inhibit differentiation through upregulation of cyclin D1. Development 2001;128:2373–2384. [PubMed: 11493556]
22. Odelberg SJ, Kollhoff A, Keating MT. Dedifferentiation of mammalian myotubes induced by msx1. Cell 2000;103:1099–1109. [PubMed: 11163185]
23. Argiropoulos B, Yung E, Humphries RK. Unraveling the crucial roles of Meis1 in leukemogenesis and normal hematopoiesis. Genes Dev 2007;21:2845–2849. [PubMed: 18006680]
24. Ouyang J, Shen YC, Yeh LK, et al. Pax6 overexpression suppresses cell proliferation and retards the cell cycle in corneal epithelial cells. Invest Ophthalmol Vis Sci 2006;47:2397–2407. [PubMed: 16723449]
25. Kunisato A, Chiba S, Nakagami-Yamaguchi E, et al. HES-1 preserves purified hematopoietic stem cells ex vivo and accumulates side population cells in vivo. Blood 2003;101(5):1777–1783. [PubMed: 12406868]
26. Perry SS, Zhao Y, Nie L, Cochrane SW, Huang Z, Sun XH. Id1, but not Id3, directs long-term repopulating hematopoietic stem-cell maintenance. Blood 2007;110:2351–2360. [PubMed: 17622570]
27. Bai G, Sheng N, Xie Z, et al. Id sustains Hes1 expression to inhibit precocious neurogenesis by releasing negative autoregulation of Hes1. Dev Cell 2007;13:283–297. [PubMed: 17681138]
28. Fleming HE, Janzen V, Lo Celso C, et al. Wnt signaling in the niche enforces hematopoietic stem cell quiescence and is necessary to preserve self-renewal in vivo. Cell Stem Cell 2008;2:274–283. [PubMed: 18371452]
29. Reya T, Clevers H. Wnt signalling in stem cells and cancer. Nature 2005;434:843–850. [PubMed: 15829953]
30. David R, Brenner C, Stieber J, et al. Mes P1 drives vertebrate cardiovascular differentiation through Dkk-1-mediated blockade of Wnt-signalling. Nat Cell Biol 2008;10:338–345. [PubMed: 18297060]
31. Bowerman B. Cell signaling: Wnt moves beyond the canon. Science 2008;320:327–328. [PubMed: 18420922]
32. Nemeth MJ, Topol L, Anderson SM, Yang Y, Bodine DM. Wnt5a inhibits canonical Wnt signaling in hematopoietic stem cells and enhances repopulation. Proc Natl Acad Sci USA 2007;104:15436–15441. [PubMed: 17881570]
33. Mikels AJ, Nusse R. Purified Wnt5a protein activates or inhibits beta-catenin-TCF signaling depending on receptor context. PLoS Biol 2006;4:e115. [PubMed: 16602827]
34. D'Acquisto F, Perretti M, Flower RJ. Annexin-A1: a pivotal regulator of the innate and adaptive immune systems. Br J Pharmacol 2008;155(2):152–169. [PubMed: 18641677]

35. Lammers T, Lavi S. Role of type 2C protein phosphatases in growth regulation and in cellular stress signaling. Crit Rev Biochem Mol Biol 2007;42:437–461. [PubMed: 18066953]
36. Lu X, Nguyen TA, Zhang X, Donehower LA. The Wip1 phosphatase and Mdm2: cracking the "Wip" on p53 stability. Cell Cycle 2008;7:164–168. [PubMed: 18333294]
37. Demidov ON, Timofeev O, Lwin HN, Kek C, Appella E, Bulavin DV. Wip1 phosphatase regulates p53-dependent apoptosis of stem cells and tumorigenesis in the mouse intestine. Cell Stem Cell 2007;16(1):180–190. [PubMed: 18371349]
38. Kawajiri K, Fujii-Kuriyama Y. Cytochrome P450 gene regulation and physiological functions mediated by the aryl hydrocarbon receptor. Arch Biochem Biophys 2007;464:207–212. [PubMed: 17481570]
39. Pereira Serafim PV, Cotrim Guerreiro da Silva ID, Manoukias Forones N. Relationship between genetic polymorphism of CYP1A1 at codon 462 (Ile462Val) in colorectal cancer. Int J Biol Markers 2008;23:18–23. [PubMed: 18409146]
40. Albert O, Edwards AO, Ritter R, et al. Complement factor H polymorphism and age-related macular degeneration. Science 2005;5720:421–424.
41. Spencer KL, Hauser MA, Olson LM, et al. Protective effect of complement factor B and complement component 2 variants in age-related macular degeneration. Hum Mol Genet 2007;16:1986–1992. [PubMed: 17576744]
42. Keyse SM. Dual-specificity MAP kinase phosphatases (MKPs) and cancer. Cancer Metastasis Rev 2008;27:253–261. [PubMed: 18330678]
43. Mandl M, Slack DN, Keyse SM. Specific inactivation and nuclear anchoring of extracellular signal-regulated kinase 2 by the inducible dual-specificity protein phosphatase DUSP5. Mol Cell Biol 2005;25:1830–1845. [PubMed: 15713638]
44. Arkell RS, Dickinson RJ, Squires M, Hayat S, Keyse SM, Cook SJ. DUSP6/MKP-3 inactivates ERK1/2 but fails to bind and inactivate ERK5. Cell Signal 2008;20:836–843. [PubMed: 18280112]
45. Tresini M, Lorenzini A, Torres C, Cristofalo VJ. Modulation of replicative senescence of diploid human cells by nuclear ERK signaling. J Biol Chem 2007;282:4136–4151. [PubMed: 17145763]
46. Caunt CJ, Rivers CA, Conway-Campbell BL, Norman MR, McArdle CA. Epidermal growth factor receptor and protein kinase C signaling to ERK2: spatiotemporal regulation of ERK2 by dual specificity phosphatases. J Biol Chem 2008;283:6241–6252. [PubMed: 18178562]
47. Maier JV, Brema S, Tuckermann J, et al. Dual specificity phosphatase 1 knockout mice show enhanced susceptibility to anaphylaxis but are sensitive to glucocorticoids. Mol Endocrinol 2007;21:2663–2671. [PubMed: 17636038]
48. Franklin CC, Kraft AS. Conditional expression of the mitogen-activated protein kinase (MAPK) phosphatase MKP-1 preferentially inhibits p38 MAPK and stress-activated protein kinase in U937 cells. J Biol Chem 1997;272:16917–16923. [PubMed: 9202001]
49. Cadalbert L, Sloss CM, Cameron P, Plevin R. Conditional expression of MAP kinase phosphatase-2 protects against genotoxic stress-induced apoptosis by binding and selective dephosphorylation of nuclear activated c-jun N-terminal kinase. Cell Signal 2005;17:1254–1264. [PubMed: 16038800]
50. Owens DM, Keyse SM. Differential regulation of MAP kinase signalling by dual specificity protein phosphatases. Oncogene 2007;26:3203–3213. [PubMed: 17496916]
51. Larderet G, Fortunel NO, Vaigot P, et al. Human side population keratinocytes exhibit long-term proliferative potential and a specific gene expression profile and can form a pluristratified epidermis. Stem Cells 2006;24:965–974. [PubMed: 16282445]
52. Avniel S, Arik Z, Maly A, et al. Involvement of the CXCL12/CXCR4 pathway in the recovery of skin following burns. J Invest Dermatol 2006;126:468–476. [PubMed: 16385346]
53. Florin L, Maas-Szabowski N, Werner S, Szabowski A, Angel P. Increased keratinocyte proliferation by JUN-dependent expression of PTN and SDF-1 in fibroblasts. J Cell Sci 2005;118:1981–1989. [PubMed: 15840658]
54. Harrington AE, Morris-Triggs SA, Ruotolo BT, Robinson CV, Ohnuma S, Hyvönen M. Structural basis for the inhibition of activin signalling by follistatin. EMBO J 2006;25:1035–1045. [PubMed: 16482217]

55. Thompson TB, Lerch TF, Cook RW, Woodruff TK, Jardetzky TS. The structure of the follistatin:activin complex reveals antagonism of both type I and type II receptor binding. Dev Cell 2005;9:535–543. [PubMed: 16198295]
56. Larouche D, Tong X, Fradette J, Coulombe PA, Germain L. Vibrissa hair bulge houses two populations of skin epithelial stem cells distinct by their keratin profile. FASEB J 2008;22:1404–1415. [PubMed: 18162489]
57. Campbell C, Risueno RM, Salati S, Guezguez B, Bhatia M. Signal control of hematopoietic stem cell fate: Wnt, Notch, and Hedgehog as the usual suspects. Curr Opin Hematol 2008;15:319–325. [PubMed: 18536569]
58. Hofmeister CC, Zhang J, Knight KL, Le P, Stiff PJ. Ex vivo expansion of umbilical cord blood stem cells for transplantation: growing knowledge from the hematopoietic niche. Bone Marrow Transplant 2007;39:11–23. [PubMed: 17164824]
59. Adolphe C, Wainwright B. Pathways to improving skin regeneration. Expert Rev Mol Med 2005;7:1–14. [PubMed: 16179092]
60. Lin HT, Chiou SH, Kao CL, et al. Characterization of pancreatic stem cells derived from adult human pancreas ducts by fluorescence activated cell sorting. World J Gastroenterol 2006;12:4529–4535. [PubMed: 16874866]
61. Brooke G, Tong H, Levesque JP, Atkinson K. Molecular trafficking mechanisms of multipotent mesenchymal stem cells derived from human bone marrow and placenta. Stem Cells Dev 2008;17 (5):929–940. [PubMed: 18564033]
62. Paré JF, Sherley JL. Biological principles for ex vivo adult stem cell expansion. Curr Top Dev Biol 2006;73:141–171. [PubMed: 16782458]
63. Tsai RJ, Li LM, Chen JK. Reconstruction of damaged corneas by transplantation of autologous limbal epithelial cells. N Engl J Med 2000;343:86–93. [PubMed: 10891515]
64. Chen YT, Li W, Hayashida Y, et al. Human amniotic epithelial cells as novel feeder layers for promoting ex vivo expansion of limbal epithelial progenitor cells. Stem Cells 2007;25:1995–2005. [PubMed: 17495107]
65. Chen Z, Li DQ, Tong L, Stewart P, Chu C, Pflugfelder SC. Targeted inhibition of p57 and p15 blocks transforming growth factor beta-inhibited proliferation of primary cultured human limbal epithelial cells. Mol Vis 2006;12:983–994. [PubMed: 16943770]

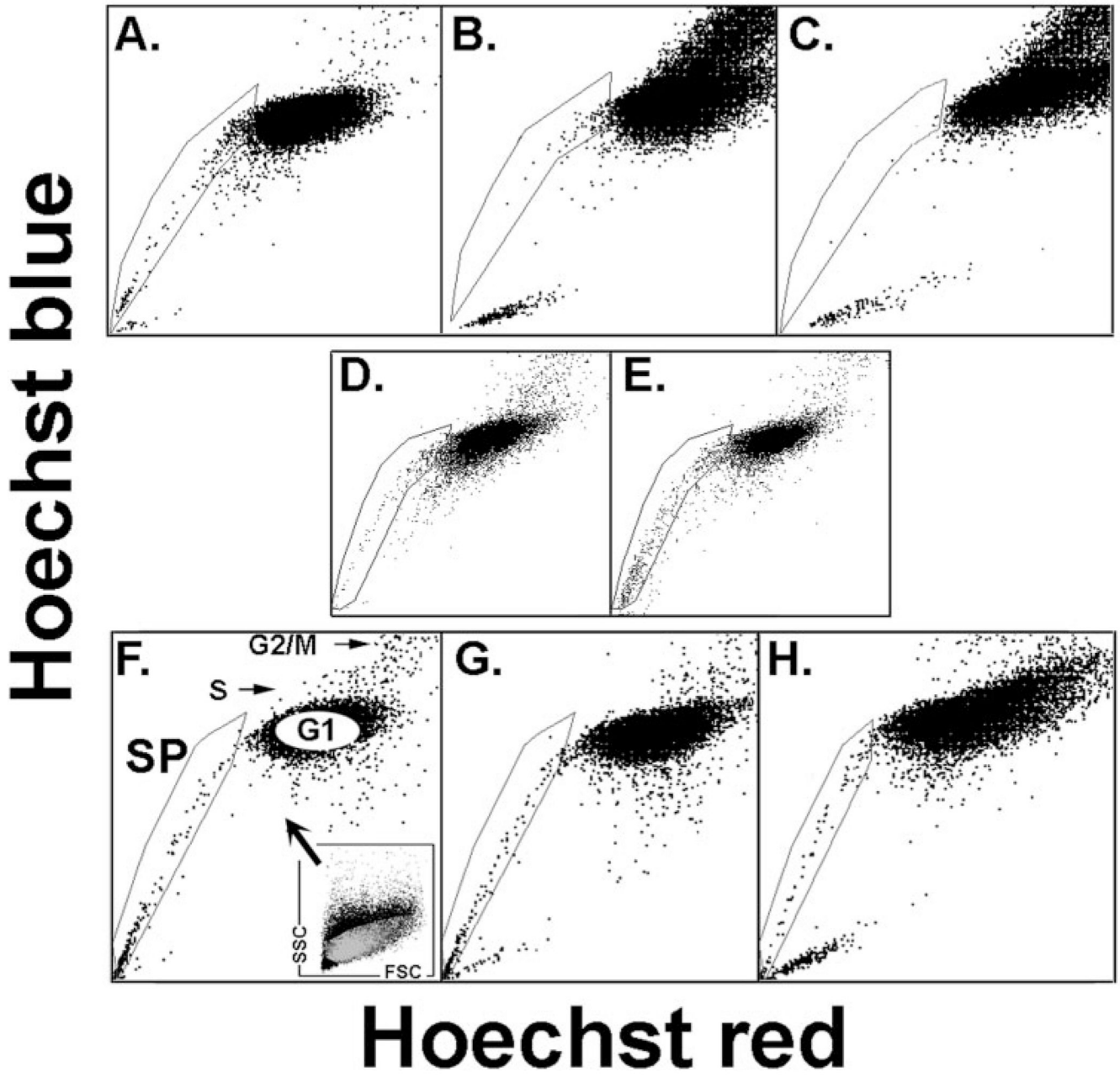

FIGURE 1.

Presence of SP cells in cultured conjunctival epithelium as a function of time in culture and medium. Rabbit cells after 16 (**A**), 40 (**B**, **D**), and 64 (**C**) hours of culture in SHEM or 40 hours in base medium (**E**). Human cells after 16 (**F**), 40 (**G**), and 64 (**H**) hours in SHEM. (**F**) Includes a description of the light-scatter gate used to exclude nonepithelial cells from the SP and nSP cohorts examined in the microarray studies. The Hoechst plot SP, G_1, S, and G_2/M are indicated.

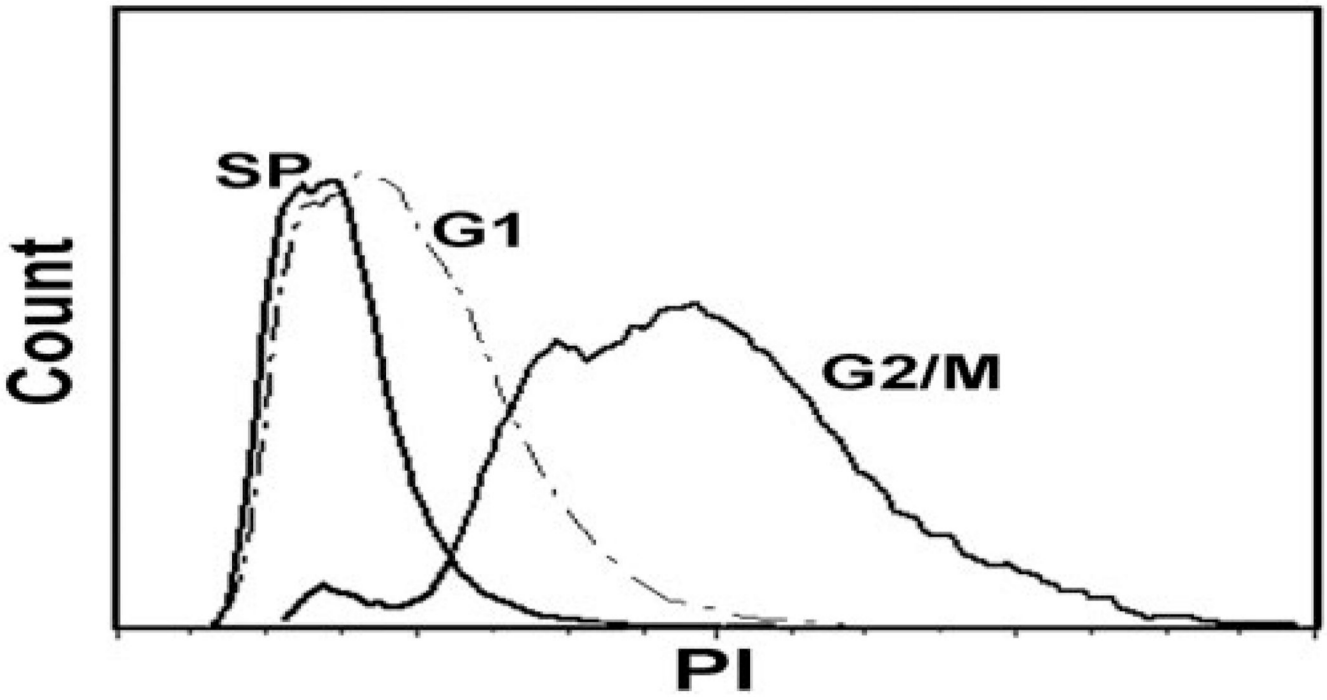

FIGURE 2.
Cycling status of rabbit CNJE cells.

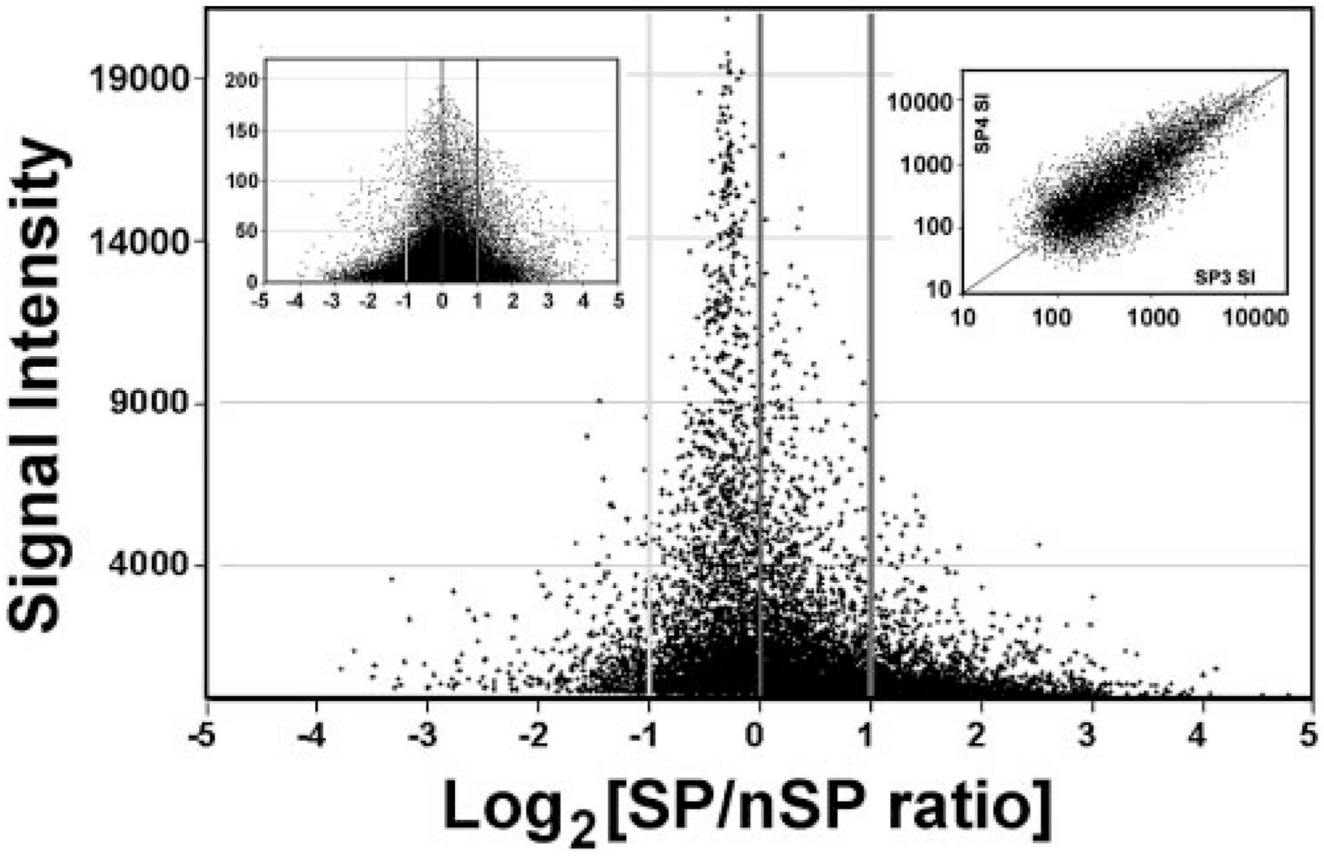

FIGURE 3.

Plot of $\log_2$ of SP/nSP ratios versus signal intensity (SI). Main frame. Expressed transcript set. Note that there are many more transcripts in the >+1 (ratio, 2) than in the >−1 range. *Left side inset*: nonexpressed transcript set. For graphic clarity SIs below 100 have been excluded. *Right side inset*: logarithmic plot of SIs for the SP cells of the first and third microarray experiment. Only SIs with a 98% confidence level (MAS5) have been included.

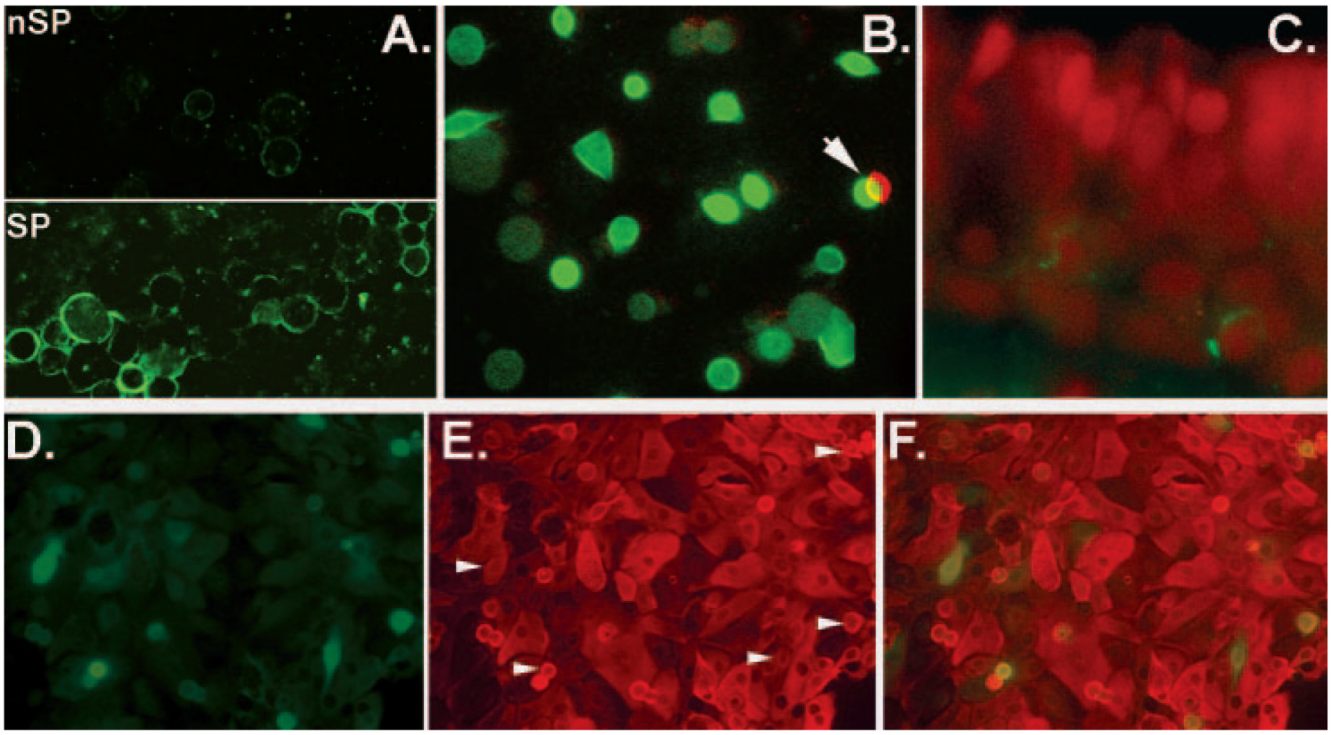

FIGURE 4.

Expression of CD62E epitopes in the CNJE. (**A**) Cytospin-sorted SP and nSP cells (SP cells aggregated before centrifugation). (**B**) Double immunostaining of a 12-hour CNJE culture on glass. *Green*: FITC-conjugated anti-keratin14 Ab; *red*: polyclonal anti-CD62E followed by Alexa Fluor 568–conjugated anti-rabbit IgG. *Green* and *red* images were superimposed with a half-cell offset. (**C**) Cryosection of HCNJE reacted with monoclonal anti-CD62E followed by Alexa 488–conjugated anti-mouse IgG and PI nuclear counterstains. (**D–F**) A 72-hour double HCNJE culture. (**D**) Anti-CD62E polyclonal Ab followed by Alexa Fluor 488–conjugated secondary Ab. (**E**) Monoclonal pan-cytokeratin Ab followed by secondary Alexa Fluor 568–conjugated secondary Ab. *Arrows*: the location of CD62-positive cells. (**F**) Merged image.

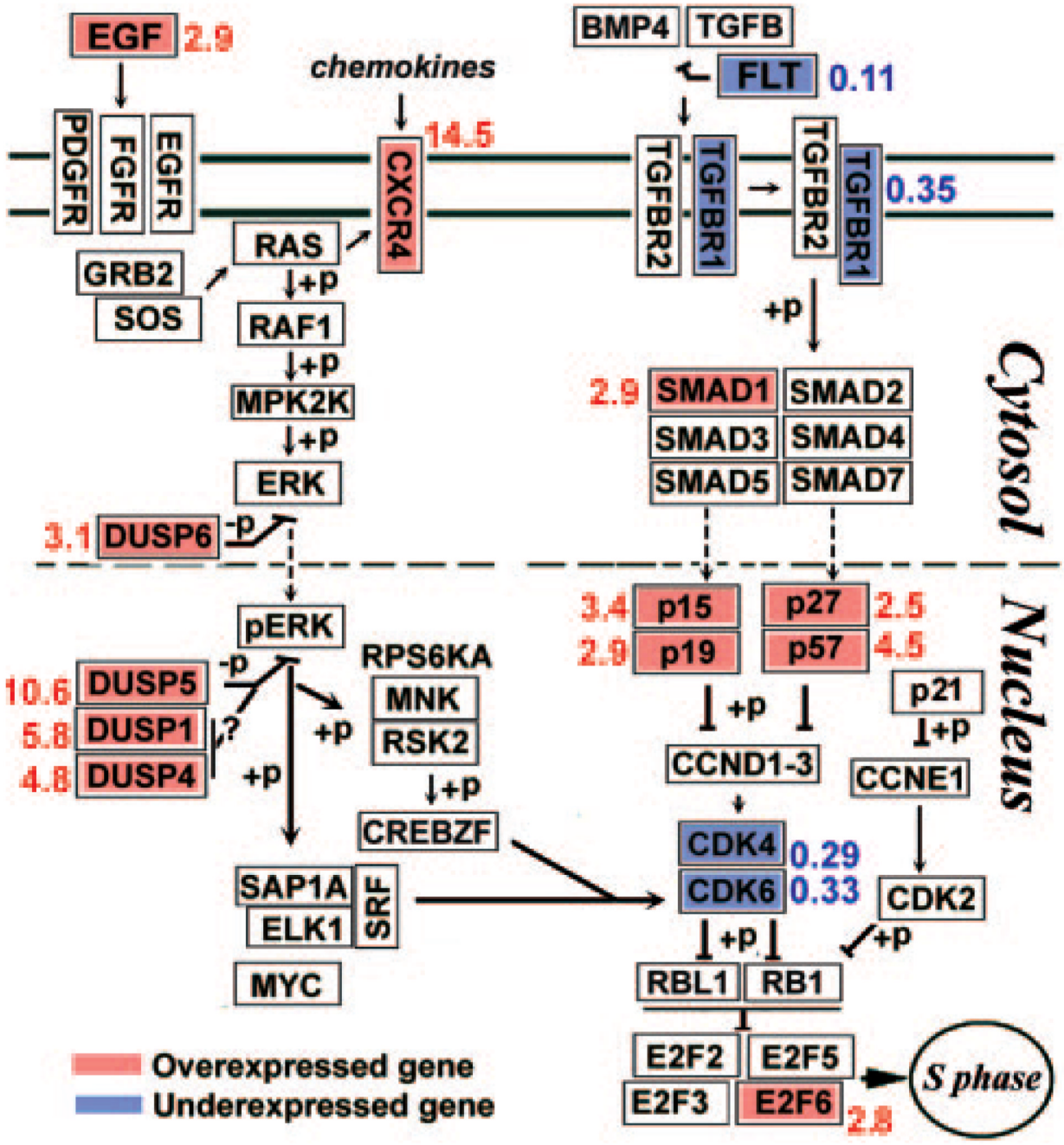

FIGURE 5.

Over- and underexpression of genes in cellular pathways affecting activity at the G_1 to S cell cycle restriction (R) point. Gen-Mapp pathways have been modified from the originals by removing genes not included in the AE gene file and highlighting genes exhibiting SP/nSP SI ratios (written next to each gene) higher than 2.5 in *red* and those with ratios smaller than 0.4 in *blue*. +p and −p indicate phospho- or dephosphorylation, respectively. Question marks next to DUSP1 and DUSP4 indicate that the activity of these two enzymes may not correlate with the inhibition of proliferation.

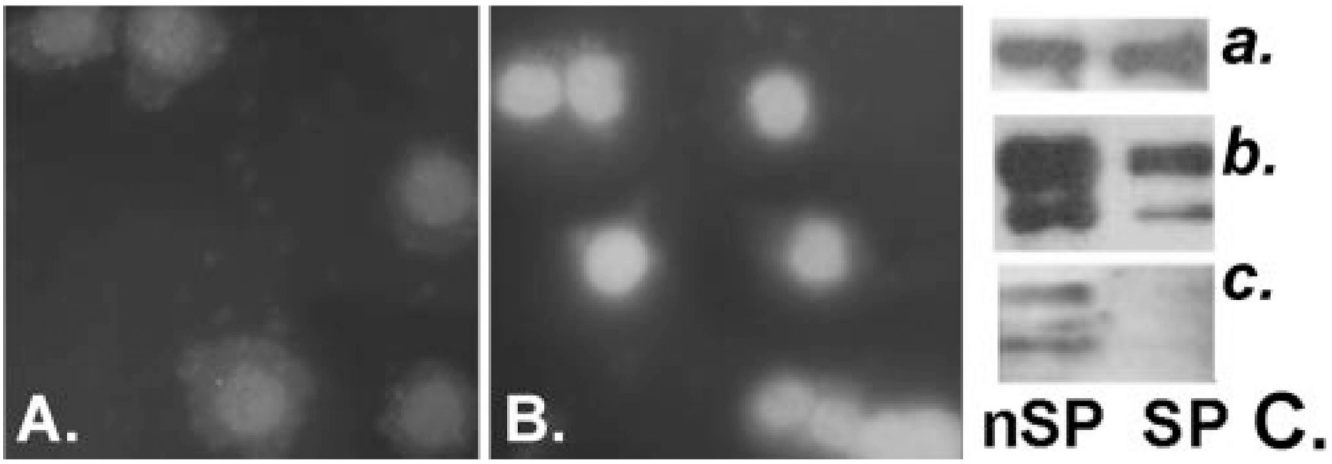

FIGURE 6.

DUSP4 and ERK expression and phosphorylation in SP and nSP cells. DUSP4 immunostaining of cytospins of HCNJE nSP (**A**) and SP (**B**) cells. (**C**) Western blot of sorted rabbit CNJE cells. *Right*: (**a**) β-actin, (**b**) ERK1/2, and (**c**) pERK1/2.

Invest Ophthalmol Vis Sci. Author manuscript; available in PMC 2009 October 10.

TABLE 1

Microarray Quality Controls

A. *GAPDH* Average Sis (*n* = 4) SI SP/nSP Ratio as a Function of Relative Distance of Probed Transcript from the Start of the RNA Message Poly A Sequence (position 1261)

GAPDH Probe Location 5′–3′/(dist. polyA)	SP-SI	SP/nSP	nSP-SI
908–1256/ (5–353)	9132	0.92	9898
493–832/(429–769)	4793	0.81	5918
87–387/(874–1164)	2159	0.93	2317

B. Number of P Calls in the SP and nSP Cells in Each Microarray-Paired Experiment

	1	2	3	4	Mean ± SD
SP-P	23854	22174	22561	22310	22725 ± 770
nSP-P	20510	20570	20032	19691	20746 ± 449
Δ(SP-nSP)	3344	1604	2529	2629	2419 ± 718

C. Signal Intensities and P and A Calls across the Microarray-Paired Experiments for the Lineage Markers

	SP		nSP	
Marker	Aver. SI	P/A-1234	Aver. SI	P/A-1234
Tyrosinase	28	AMAA	17	AAPA
CD45	18	PAAP	12	AAAA
CD1a	16	AAAA	31	AAAA
ΣKeratins	3384		3485	

TABLE 2

Comparison of SP/G_1 Expression Ratios Calculated from a qPCR Experiment and from the Microarray Study

Gene	SP Ct	PCR SP/G1	Microarray SP/G1
β-Actin	23.06	1.00	1.00
CXCR4	35.90	35.57	14.51
DUSP4	31.35	23.42	5.59
DUSP5	27.68	43.44	10.61
MAP3K8	31.99	6.70	10.81
CDK4	33.62	0.02	0.29
CCND1	28.59	2.55	1.67
CCND2	33.30	0.39	0.22
CCND3	33.14	3.91	2.50
CDKN2B (P15)	25.23	24.60	3.38
CDKN1C (P57)	36.22	3.14	4.38
CDKN1B (P27)	29.68	2.07	2.43

TABLE 3

Genes for Which SP/nSP or nSP/SP SI Ratios Are Larger Than 10

Gene	Symbol	SP-SI	SP/nSP	Annotations
A. SP > nSP				
E-selectin/CD62E/ELAM 1	*SELE*	1260	141.81	Heterologous cell adhesion
Splicing factor, arginine/serine-rich 3	*SFRS3*	511	27.11	pre-mRNA splicing factor
CD93	*CD93*	264	23.17	Heterologous cell adhesion
E74-like-3	*ELF3*	3683	17.26	Epithelial nuclear transcription factor
Potassium voltage-gated channel, Isk-rel., 3	*KCNE3*	857	14.95	Regulation of K_ channel
Chemokine (C-X-C motif) receptor 4	*CXCR4*	367	14.51	Growth and motility receptor
Zinc finger and BTB domain containing 10	*ZBTB10*	618	14.20	Nuclear transcription factor
Heterogeneous nuclear ribonucleoprot. D	*HNRPD*	369	13.79	pre-mRNA processing and stabilization
Prot. phosphatase 1D mag.-dep., delta iso.	*PPM1D*	677	12.94	Regulation of p53 induced apoptosis (stem)
Methyltransferase-like 7A	*METTL7*	816	12.77	Methyl transferase precursor
Annexin A1	*ANXA1*	525	12.55	PLA-2 inhibitor-Inflammation inhib.
Cytochrome P450, family 1 A, pol 1	*CYP1A1*	275	12.36	Xenobiotic aromatic processing
Histone Cluster 1, H4h	*HIST1H*	689	11.99	Histone
Statherin	*STATH*	1288	11.97	Secreted salivary protein
Myosin regulatory light chain interacting protein	*MYLIP*	1240	11.59	Inhibitor of cell motility (neurites)
Zinc finger protein 750	*ZNF750*	365	11.21	Nuclear transcription factor
Colony stimulating factor 2 receptor, beta	*CSF2RB*	102	11.07	Granulocyte-macrophage growth receptor
Histone cluster 1, H2bg	*HIST1H*	284	10.86	Histone
MAP kinase kinase kinase 8	*MAP3K*	1478	10.81	MAPK pathway mediator
Dual specificity phosphatase 5	*DUSP5*	4262	10.61	Dephosphorylation of ERK
Cytochrome P450, family 26-A polypeptide 1	*CYP26A1*	1194	10.48	Retinoic acid processing
B. nSP > SP				
Collagen, type XVII, alpha 1	*COL17A1*	302	31.79	Cell-matrix adhesion
Transgelin	*TAGLN*	1308	25.1	Cytoskeleton organization
Parathyroid hormone-like hormone	*PTHLH*	1036	20.13	Differentiation (mammary gland)
Podoplanin	*PDPN*	1352	18.56	Phyllopodia-dependent cell motility
Dickkopf 3	*DKK3*	1172	16.35	Negative regulation WNT signaling
Caldesmon 1	*CALD1*	5025	12.74	Cell motility
Secretogranin V	*SCG5*	576	12.4	Secreted protein-unknown function
Dystonin	*DST*	1804	11.98	Cytoskeleton organization
Matrix metallopeptidase 9	*MMP9*	2090	11.27	Peptido-glycan digestion
TGFbeta 1 induced transcript 1	*TGFB111*	355	11.2	Focal adhesion adapter
Interleukin 13 receptor, alpha 2	*IL13RA2*	11453	10.14	Interleukin receptor

Gene	Symbol	SP-SI	SP/nSP	Annotations

TABLE 4

Overrepresented Ontological Terms in the Gene Lists

Category	Term	*P*
Overexpressed		
SP_PIR_KEYWORDS	Nuclear protein	1.47E-40
SP_PIR_KEYWORDS	Transcription	1.15E-31
SP_PIR_KEYWORDS	Zinc-finger	5.23E-31
SP_PIR_KEYWORDS	metal-binding	2.19E-29
SP_PIR_KEYWORDS	Transcription regulation	3.45E-29
SP_PIR_KEYWORDS	DNA-binding	4.56E-23
GOTERM_MF_ALL	Transition metal ion binding	2.89E-21
GOTERM_MF_ALL	Zinc ion binding	7.83E-20
GOTERM_MF_ALL	Transcription factor binding	1.59E-09
UP_SEQ_FEATURE	Zinc finger: C2H2- type 1, 2, 3 or 4	<2.34E-08
GOTERM_MF_ALL	Transcription cofactor activity	3.76E-08
Underexpressed		
GOTERM_MF_ALL	Actin binding	8.34E-09
SP_PIR_KEYWORDS	Cytoskeleton	6.03E-09
GOTERM_BP_ALL	Cell organization and biogenesis	2.96E-08
GOTERM_MF_ALL	Cytoskeletal protein binding	2.94E-07
SP_PIR_KEYWORDS	Extracellular matrix	5.09E-07
GOTERM_BP_ALL	Protein intracell. transport/localization	5.50E-05

TABLE 5

Substantially Over- or Underexpressed Homeodomain and Development-Related Genes

Affymetrix ID	Gene Symbol	SP-SI	SP/nSP
205932_s_at	*MSX1*	191	8.24
204069_at	*MEIS1*	779	5.10
203394_s_at	*HES1*	1234	9.02
208937_s_at	*ID1*	1093	7.95
207826_s_at	*ID3*	1392	4.41
201566_x_at	*ID2*	2845	4.11
205990_s_at	*WNT5A*	337	4.06
221245_s_at	*FZD5*	924	4.29
214247_s_at	*DKK3*	72	0.06
	ALL DKK		0.21
235795_at	*PAX6*	2875	8.10
228347_at	*SIX1*	1002	6.09